JOURNAL OF SOLID STATE CHEMISTRY 97, 274–282 (1992)

Preparation and Investigation of the Physical Properties of Fluorinated $Nd_{2-x}Sr_xNiO_{4+\delta}$

B. W. ARBUCKLE, K. V. RAMANUJACHARY,
A. M. BUCKLEY, AND M. GREENBLATT*

Department of Chemistry, Rutgers—The State University of New Jersey, Piscataway, New Jersey 08855-0939

Received July 8, 1991

Selected members of the $Nd_{2-x}Sr_xNiO_{4+\delta}$ solid solution series were fluorinated by a low temperature ion-exchange reaction. $Nd_2NiO_{4.16}$ is orthorhombic at ambient temperature and shows an increase in the orthorhombic distortion as a result of fluorination. The *a* unit cell parameter of $Nd_2NiO_{4.16-x}F_y$ decreases while the *b* and *c* cell parameters increase relative to the oxygen rich sample $Nd_2NiO_{4.16}$. The unit cell volume of the fluorinated sample relative to the oxygen rich sample increases. $Nd_2NiO_{4.16}$ undergoes a structural phase transition at 575°C, and the fluorinated analogue shows no evidence of a structural phase transition up to 700°C. The $Nd_2NiO_{4.16-x}F_y$ phase decomposes at 700°C into $Nd_2NiO_{4+\delta}$, NdOF, NdF_3, and NiO as determined by differential thermal analysis and X-ray diffraction analysis. The significant changes in the electrical and magnetic properties of fluorinated $Nd_{2-x}Sr_xNiO_{4+\delta}$ compared to the oxide are discussed in terms of structural properties of the Ni–O basal planes.

Introduction

Rare earth transition metal mixed oxides of the type A_2BO_4 (A = rare earth, B = transition metal), with the tetragonal K_2NiF_4-type structure, are composed of alternating perovskite (ABO_3) and rock salt (AO) layers along the tetragonal *c*-axis (Fig. 1). The *B*–O octahedra share corners in the *ab* plane forming a two-dimensional array of *B*–O–*B* bonds which give these compounds quasi-two-dimensional magnetic and electrical properties (*1–4*). It is well known that the physical properties of perovskite-related compounds can be manipulated by adjusting the valence of the transition metal ion. For example, the antiferromagnetic semiconductor La_2CuO_4 can be made superconducting by either the systematic substitution of divalent cations, such as Sr^{2+} and Ba^{2+}, into the La^{3+} sites or by the introduction of oxygen interstitials into the crystal lattice (*5*). In both cases electrons are partially removed from the Cu–O plane which results in a formal $Cu^{2+/3+}$ mixed valency. The antiferromagnetic semiconductor Nd_2CuO_4, which has a modified K_2NiF_4 structure, can also be transformed into a high temperature superconductor by the partial substitution of Ce^{4+} for Nd^{3+}. Substitution of Ce^{4+} for the Nd^{3+} adds electrons to the Cu–O plane which partially reduces the oxidation state of copper and result in a formal $Cu^{2+/1+}$ mixed valency. Superconductivity has been reported in $Nd_2CuO_{4-x}F_x$ (*6*). Fluorination,

---

* To whom correspondence should be addressed.

0022-4596/92 $3.00

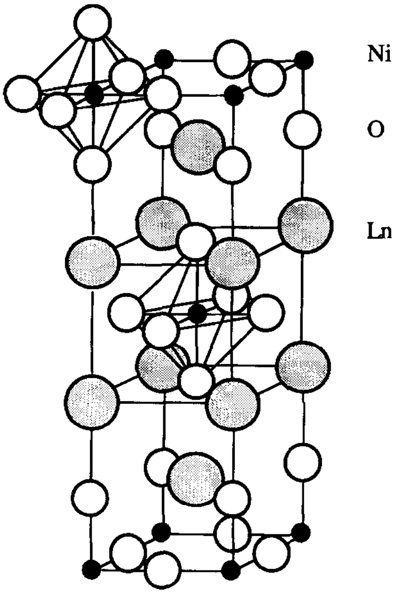

FIG. 1. Unit cell of the Nd_2NiO_4 structure.

like Ce^{4+} substitution, leads to partial reduction of the copper valence. The structural similarity between Ln_2NiO_4 (Ln = La^{3+}, Pr^{3+}, Nd^{3+})-type compounds and the superconducting La_2CuO_4 types, coupled with recent reports of possible superconductivity in the $La_{2-x}Sr_xNiO_{4+\delta}$ system (*7, 8*), has generated considerable efforts to evaluate the physicochemical properties of the Ln_2NiO_4 class of compounds.

Rare earth nickelates show a range of oxygen nonstoichiometry depending upon their synthetic preparation and this is manifested in various structural distortions from the ideal tetragonal symmetry. The presence of excess oxygen in these structures and a strong correlation between structural stability and oxygen content have been established by several investigators (*9*). Moreover, the electronic and magnetic properties of $Ln_2NiO_{4+\delta}$-type compounds are extremely sensitive to deviations in the oxygen stoichiometry (*10–12*). For example, stoichiometric Nd_2NiO_4 is unstable in air and reacts with atmospheric moisture to form hydroxy-carbonates under ambient conditions (*13*). Nonstoichiometric $La_2NiO_{4+\delta}$ is tetragonal at ambient temperatures while the nearly stoichiometric sample (δ = 0) shows an orthorhombic distortion. Electrical conductivity studies on $La_2NiO_{4+\delta}$ reveal a semiconductor-to-metal transition between 500 and 620 K (*3, 14*). Recently we have reported on the $Nd_{2-x}Sr_xNiO_{4+\delta}$ solid solution series (*15*). For $x < 0.2$ the samples are orthorhombic and undergo a structural phase transition to tetragonal symmetry as the Sr^{2+} content exceeds $x = 0.2$. The orthorhombic samples incorporate excess oxygen into their structures, which presumably helps to stabilize the orthorhombic phase; the tetragonal samples are always found to be stoichiometric in oxygen (δ = 0). For $Nd_2NiO_{4+\delta}$ the δ value is 0.16 ± 0.03 (*15*). The excess oxygens can occupy interstitial sites located between two rock salt NdO planes, similar to that observed for $La_2NiO_{4.18}$ (*9*). $Nd_2NiO_{4+\delta}$ can be easily reduced to $Nd_2NiO_{4.0}$ under mild reducing conditions at 275°C and reversibly oxidized back to the oxygen rich sample in air at 100°C (*13*). It is apparent that the excess oxygen in $Nd_2NiO_{4+\delta}$ is fairly mobile and can be reversibly removed and incorporated.

Substitution of fluorine for oxygen in rare earth transition metal oxide materials is not as extensive as one might expect considering the similarity in size of the O^{2-} (1.400 Å) and F^- (1.333 Å) ions. In order to maintain charge neutrality, replacement of O^{2-} by F^- in Ln_2NiO_4 must be accompanied by either a change in the cationic charge or the proper ratio of F^- for O^{2-} substitution. If the *B* cation can exhibit variable oxidation states then a one-to-one F^- for O^{2-} substitution is possible; otherwise, the substitution ratio must be two F^- for one O^{2-}. Typical preparation techniques employed in the synthesis of oxyfluorides with perovskite-related structures involve a direct solid state reaction between the metal oxides and fluorides (*16–18*). Recently there have been reports on the preparation of $La_{2-y}Dy_yCuO_{4-x}F_{2x}$ using a simple ion-exchange reaction (*19, 20*). We report here the fluorination of $Nd_{2-x}Sr_xNiO_{4+\delta}$-type compounds by a similar low temperature ion-exchange reaction.

Experimental

Pellets of the parent compounds $Nd_2NiO_{4.16}$, $Nd_{1.5}Sr_{0.5}NiO_{4.0}$, and $NdSrNiO_{4.0}$ were prepared as reported earlier (*15*). Single-phase $Nd_{2-x}Sr_xNiO_{4+\delta-x}F_y$ samples, as determined from powder X-ray diffraction (PXD), were prepared by a procedure previously reported with modification (*19, 20*). Typically, the pellets of $Nd_{2-x}Sr_xNiO_{4+\delta}$ were placed into a glass tube containing ZnF_2 in molar ratios of sample to ZnF_2 of 4 : 1. The samples were separated from ZnF_2 by glass wool. Special care was taken to control the volume and pressure inside the sealed glass tube in order to ensure that the reaction conditions were identical for different preparations. The ampoules were initially outgassed to a final pressure of P = 0.10 atm prior to sealing and were heated at 295°C for 48 hr. Following this treatment the ampoules were opened and the samples were annealed in air at 400°C for 24 hr. The structural and thermal properties of the resultant black pellets were examined by PXD and differential thermal analysis (DTA). The total fluorine content of the fluorinated samples was analyzed electrochemically by Schwarzkopf Microanalytical Laboratory with a fluorine-ion-selective electrode. Oxygen-deficient samples of $Nd_2NiO_{4.16-x}$ were prepared by annealing $Nd_2NiO_{4.16}$ under 5% H_2/He at 285°C for 2–4 hr.

Powder X-ray diffraction data were obtained with a Scintag Pad V diffractometer with monochromatized Cu$K\alpha$ radiation. Least-square refinement of the observed powder diffraction data was used to evaluate the unit cell parameters. The d spacings were corrected for systematic errors by calibration with mica. Electrical resistivities of the samples were measured by a standard four-probe technique with a DE202 cryostat (APD Cryogenics) from room temperature to 15 K. A Squid magnetometer (Quantum Design) was used to measure the magnetic susceptibility of samples in the range 2–370 K at an applied magnetic field of 1000 G. The total oxygen content was determined by iodometric titration and when appropriate by hydrogen reduction with a DuPont 951 thermogravimetric analyzer; the sample was placed in a silver pan and heated in flowing 5% H_2 in helium gas (0.1 liter/min) to 1000°C at 10°C/min.

The morphology of the specimens was examined with an Amrek scanning electron microscope on as-prepared and fractured surfaces. Energy dispersive X-ray analysis was performed on randomly selected grains to verify compositional homogeneity, across the grains. Samples were also examined using a JEOL 100CX transmission electron microscope at an accelerating voltage of 100 kV. The powdered samples were ground well and sprinkled onto 200 mesh Formvar/carbon-coated copper grids. The grids were gently tapped to remove excess material. Selected area electron diffraction patterns were obtained for several crystallites. The diffraction constant of the microscope was calibrated using a MoO_3 standard.

Results and Discussion

Structure

Initial evidence that fluorination of $Nd_2NiO_{4.16}$ was occurring by the low temperature ion-exchange reaction was indicated by the conversion of ZnF_2 to ZnO as determined by PXD. The total fluorine content in each of the samples studied is presented in Table I. The distribution of F^- was found to

TABLE I

STRUCTURAL PROPERTIES OF $Nd_{2-x}Sr_xNiO_{4+\delta}$ AND $Nd_{2-x}Sr_xNiO_{4-y}F_y$

Compound	a (Å)	b (Å)	c (Å)	V (Å^3)	c/a_t
$Nd_2NiO_{4.16\pm0.03}$[a]	5.378(1) (3.825)[b]	5.441(1)	12.355(1)	361.52(7) (180.76)[c]	— (3.230)[c]
$Nd_2NiO_{4.16-x}F_y$ ($y \sim 0.018$)	5.287(1) (3.831)[b]	5.548(1)	12.411(3)	364.01(8) (182.13)[c]	— (3.240)[c]
$Nd_2NiO_{4.08\pm0.03}$	5.383(1) (3.828)[b]	5.445(1)	12.342(2)	361.74(7) (180.88)[c]	— (3.224)[c]
$Nd_2NiO_{4.0}$[d]	5.3814(2) (3.8772)[b]	5.5850(2)	12.1143(4)	364.09(3) (182.05)[c]	(3.124)[c]
$Nd_{1.5}Sr_{0.5}NiO_{3.98\pm0.03}$[a]	3.776(1)		12.473(3)	177.81(4)	3.305
$Nd_{1.5}Sr_{0.5}NiO_{3.98-x}F_y$ ($y \sim 0.024$)	3.773(1)		12.483(2)	177.70(5)	3.308
$NdSrNiO_{4.00\pm0.03}$[a]	3.796(1)		12.303(2)	177.28(3)	3.240
$NdSrNiO_{4.00-x}F_y$ ($y \sim 0.08$)	3.794(1)		12.320(3)	177.33(5)	3.247

[a] After Ref. (15).

[b] The a_t for the orthorhombic samples were calculated using the expression $a_t = (a + b)/2\sqrt{2}$.

[c] Values for the orthorhombic samples were calculated using a_t instead of a.

[d] After Ref. (13).

be uniform throughout the bulk of the sample as determined by energy dispersive X-ray analysis. The electron diffraction patterns from several crystallites of both fluorinated and nonfluorinated compositions have been examined and a typical selected area diffraction pattern from a crystallite of $NdSrNiO_{4-x}F_y$ is shown in Fig. 2. There was no evidence of amorphous regions in any of the compositions studied, which indicates that the crystallinity of the samples remains unaffected by the incorporation of fluorine in the structure. This observation contrasts with similar studies on the fluorinated compositions of $YBa_2Cu_3O_7$, in which substantial amounts of amorphous phases have been detected by electron diffraction (*21*).

The oxygen-rich $Nd_2NiO_{4.16}$ is an orthorhombically distorted variant of the tetragonal K_2NiF_4-type structure (*22*). The orthorhombic distortion manifests itself in the splitting of some of the reflections in the PXD pattern. Figure 3A shows that for $Nd_2NiO_{4.16}$ the (020)–(200) and (024)–(204) doublets are well resolved. After this sample is fluorinated the splittings of these reflections increase dramatically as shown in Fig. 3B. The (113) and (020) reflections slightly overlap as do the (115) and (006) peaks. The (024) peak lies underneath the (115) and (006) peaks. Saez-Puche *et al.* reported similar observations when the oxygen-rich sample $Nd_2NiO_{4+\delta}$ was reduced to stoichiometric $Nd_2NiO_{4.0}$ (*13*). They attributed the observed increase in the splittings of these reflections to increased orthorhombic strain in the structure. The unit cell parameters of $Nd_2NiO_{4.16-x}F_y$, as determined from the least-square refinement of the PXD data, are presented in Table I. Relative to the oxygen-rich sample $Nd_2NiO_{4.16}$, the a cell parameter of the fluorinated sample decreases while the b and c cell dimensions increase. However, a comparison of the trends in cell parameter variations between the nearly stoichiometric $Nd_2NiO_{4.0}$ and the fluorinated $Nd_2NiO_{4.16}$ revealed significant

FIG. 2. Selected area diffraction pattern of $NdSrNiO_{4-x}F_y$ crystallite ([111] zone axis).

differences (Table I). The orthorhombic strain (defined as $s = 2(b - a)/(a + b)$), as calculated from the observed unit cell parameters, shows that the strain increases fourfold from 0.012 for the oxygen-rich samples to 0.048 for the fluorinated sample. The $Nd_2NiO_{4.0}$ sample has a calculated orthorhombic strain of 0.037 (*13*). These observations strongly indicate that the incorporation of F^- ions in $Nd_2NiO_{4.16}$ results in dramatic enhancement of the orthorhombic strain.

As mentioned earlier, $Nd_2NiO_{4.16}$ can easily be made stoichiometric under mild reducing conditions. It is conceivable that $Nd_2NiO_{4.16}$ loses oxygen under reduced pressure; the extra oxygen released could react with ZnF_2 to form ZnO. This could also explain the increase in the orthorhombic strain and the observed peak splittings. To test this hypothesis, we have repeated the experiment with Zr in place of ZnF_2, which is an excellent "oxygen-getter." In fact, we were able to reduce $Nd_2NiO_{4.16}$ by using Zr. The oxygen stoichiometry of the samples was very hard to control and ranged from $Nd_2NiO_{4.12\pm0.02}$ to $Nd_2NiO_{4.08\pm0.02}$ as determined by iodometric titration. However, the PXD of the samples did not show the large splitting of the (020)–(020) and (024)–(204) reflections observed for the fluorinated samples; moreover, these samples were easily converted back to $Nd_2NiO_{4.16}$ by annealing in air at 400°C for 24 hr. This is in contrast to the $Nd_2NiO_{4.16-x}F_y$ samples which were unchanged after heat treatment in air at 400°C for 24 hr as evident from their PXD patterns. Reac-

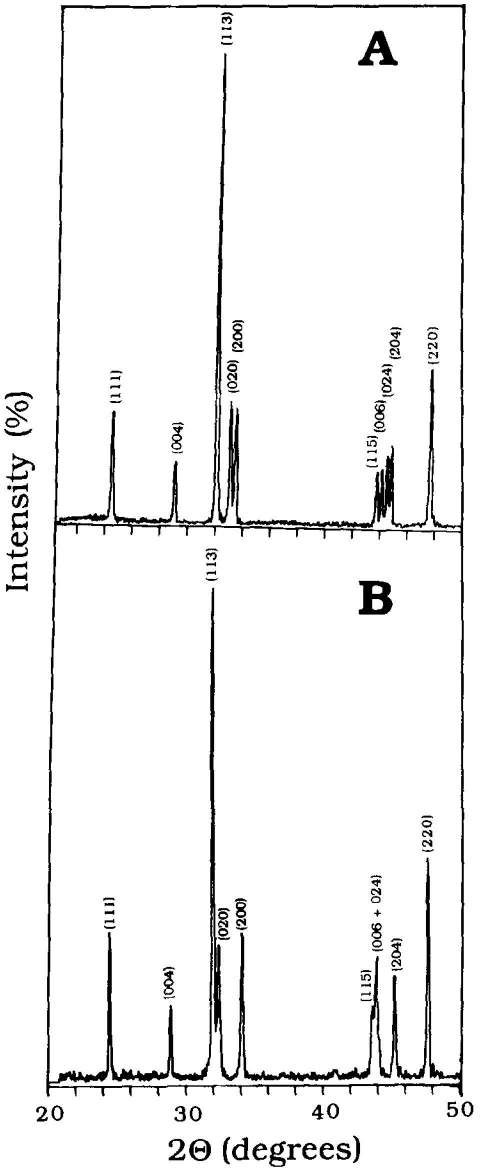

FIG. 3. Powder X-ray diffraction patterns of Nd$_2$NiO$_{4+\delta}$ (A) as prepared and (B) after fluorination.

tions of Nd$_2$NiO$_{4.16}$ in sealed tubes without ZnF$_2$ showed no evidence of reduction.

Nd$_2$NiO$_{4.16}$ undergoes a reversible structural phase transition from orthorhombic to tetragonal symmetry at 575°C (*15, 23*). We have carried out detailed DTA and high temperature X-ray diffraction studies, and find no evidence for a phase transition of the fluorinated samples below 700°C. However, Nd$_2$NiO$_{4.16-x}$F$_y$ does show an irreversible phase disproportionation at 700°C as determined by DTA and PXD. The PXD analysis of samples heated above 700°C showed the presence of Nd$_2$NiO$_{4+\delta}$, NiO, NdF$_3$, and NdOF. This implies that the fluorinated samples are inherently unstable at temperatures greater than 700°C. This is similar to what was reported for the compounds Nd$_2$CuO$_{4-x}$F$_y$ and La$_{2-y}$Dy$_y$CuO$_{4-x}$F$_{2x}$ (*6, 20*), which decomposed on heating above 900°C.

Lightfoot *et al.* (*20*) reported that La$_{1.25}$Dy$_{0.75}$CuO$_{4.0}$, which has a tetragonal T* structure (hybrid derived from the La$_2$CuO$_4$ (T) and Nd$_2$CuO$_4$ (T′) structure types with a square-pyramidal coordination of copper sandwiched between a rock-salt-like La$_2$O$_2$ and a fluorite-like Nd$_2$O$_2$ layer), undergoes an orthorhombic distortion upon fluorination. The degree of orthorhombic distortion was a function of the amount of F$^-$ incorporated into the structure. They assumed that the F$^-$ ions occupy the interstitial sites of the La$_2$O$_2$ rock salt layers in a manner similar to the extra oxygens in the related T structure of La$_2$NiO$_{4.18}$ (*9*). La$_2$NiO$_{4.18}$ exhibits an orthorhombic superstructure, $\sqrt{2}a \times \sqrt{2}a \times c$, induced by the incorporation of the interstitial oxygens between the two (001) rock salt LaO planes. The interstitial oxygen repels the four nearest neighbor apical oxygens and displaces them from the axial positions. Lightfoot *et al.* have argued along similar lines to explain the orthorhombic strain in La$_{1.25}$Dy$_{0.75}$CuO$_{4-x}$F$_{2x}$. However, they could not unambiguously determine the origin of the orthorhombic distortion from neutron diffraction data due to the inability to distinguish between O and F in the structure refinement. They proposed that the distortion might be related to the cooperative twisting of the displaced apical oxygens about the

c-axis through their neighboring interstitial anions. This would minimize the anion–anion repulsions between neighboring oxygen ions and result in an orthorhombic distortion. A similar argument may be applied to the present system. The F^- anions in the interstitial sites could interact with and repel the apical anions of the NiO_6 octahedra away from their ideal axial positions causing a cooperative tilting of the NiO_6 octahedra.

If in the present system the F^- ions were replacing the oxygens stoichiometrically (i.e., one to one) in the interstitial sites between the rock salt NdO planes of the Nd_2O_2 layers of $Nd_2NiO_{4.16}$, then the anion–anion repulsion between the interstitial anion and the apical anion would be expected to decrease. Consequently, the orthorhombic distortion would also be expected to decrease. On the other hand, assuming that the replacement by F^- is greater than one to one as reported for $La_{2-y}Dy_yCuO_{4-x}F_{2x}$, then the anion–anion repulsion should increase, resulting in an increase in the orthorhombic strain of the unit cell.

Alternatively, the increase in the orthorhombic strain could also be understood in terms of Nd^{3+} defects in the structure. The F^- anions deposited on the surface of $Nd_2NiO_{4.16}$ could leach out Nd^{3+} from the structure by forming an amorphous layer of NdOF on the surface. This would leave Nd^{3+} defects in the structure, which in turn might explain the observed orthorhombic strain. Attempts to prepare Nd^{3+}-deficient compounds, $Nd_{2-x}NiO_{4+\delta}$ ($0 < x < 0.2$), by conventional solid state reaction and/or the codecomposition of metal nitrates proved unsuccessful. This suggests that the $Nd_{2-x}NiO_4$ phases are not stable. Hence, it is unlikely that Nd^{3+} defects are the source of the observed orthorhombic strain.

Fluorination of $Nd_{1.5}Sr_{0.5}NiO_{4.0}$ and $NdSrNiO_{4.0}$ was also performed. PXD data of the resulting compounds did not show large changes in the unit cell parameters (Table I). The a cell parameter does not change significantly while the c cell parameter increases slightly. Both samples decompose above 700°C.

Electrical and Magnetic Properties

The room temperature resistivity (ρ_{RT}) of all three fluorinated compositions increased relative to the corresponding parent compound. This can be explained in part by electronegativity considerations. The F^- anion could act as a potential trapping site for electrons, thus impeding the flow of electrons; the incorporation of F^- in the Ni–O basal planes of the NiO_6 octahedra cannot be ruled out. The temperature de-

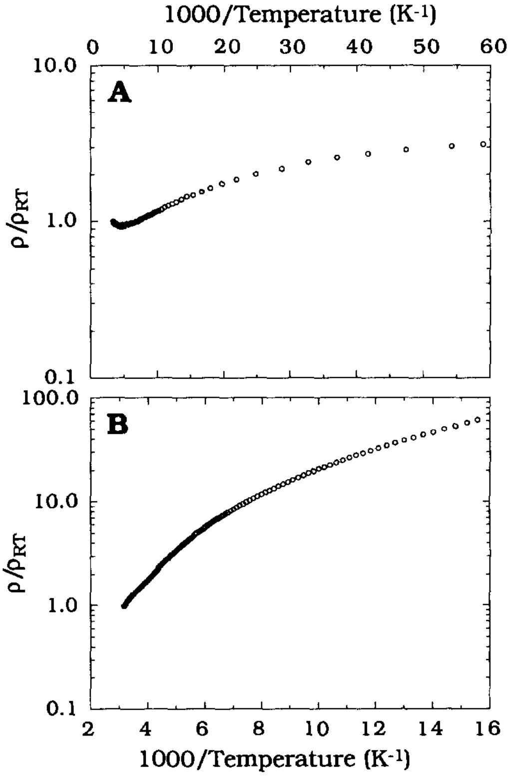

FIG. 4. Arrhenius plots of the electrical resistivity for $NdSrNiO_4$ (A) as prepared and (B) after fluorination.

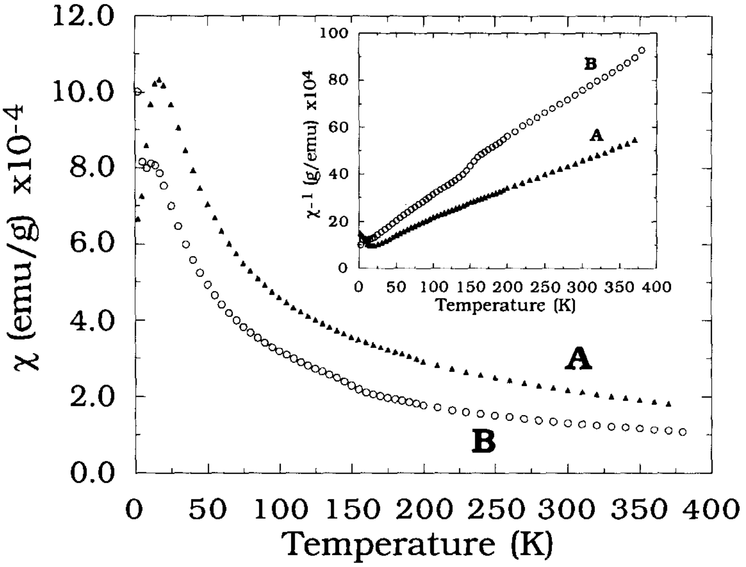

FIG. 5. Magnetic susceptibility as a function of temperature for Nd$_{1.5}$Sr$_{0.5}$NiO$_4$ (A) as prepared and (B) after fluorination. Inset shows the inverse susceptibility variations with temperature.

pendence of the resistivity of the fluorinated samples shows semiconducting behavior down to 50 K. It is interesting to note that the metallic behavior observed for NdSrNiO$_4$ (15) above 190 K disappears after fluorination (Fig. 4).

In the solid solution series Nd$_{2-x}$Sr$_x$NiO$_{4+\delta}$, the magnetic susceptibility (χ) shows Curie–Weiss behavior with the onset of long-range antiferromagnetic ordering (T_N = 17 K) in some of the intermediate members (*15*). There is no evidence for long-range magnetic order down to 2 K in all three of the fluorinated samples. The long-range antiferromagnetic order of Nd$_{1.5}$Sr$_{0.5}$NiO$_4$ appears to be frustrated upon fluorination (Fig. 5). The χ vs T plot of Nd$_{1.5}$Sr$_{0.5}$NiO$_{4-x}$F$_y$ begins to flatten out at 14 K and does not show any clear indication of long range magnetic ordering. However, a clear anomaly at 155 K in the $1/\chi$ vs T plot of Nd$_{1.5}$Sr$_{0.5}$NiO$_{4-x}$F$_y$ is seen in Fig. 5 (inset). Similar observations were reported by Saez-Puche *et al.* for stoichiometric La$_2$NiO$_4$ (*24*), which they attributed to the presence of weak ferromagnetic components due to the spin canting of the antiferromagnetically ordered Ni^{2+} as a result of a reversible structural phase transition at about 80 K. The same phenomenon was also observed for stoichiometric Nd$_2$NiO$_4$ and Pr$_2$NiO$_4$ at 90 and 120 K, respectively (*13*). This implies that the incorporation of fluorine reduces the correlation lengths of the exchange interactions causing severe distortion in the local coordination of the cations, which frustrate the antiferromagnetic ordering of the rare earth ions. This indicates that the F$^-$ is indeed being incorporated into the Nd–O rock salt layer and not the Ni–O layer. Buttrey and Honig (*4*) showed that the magnetic order of the nickel sublattice in Pr$_2$NiO$_{4+\delta}$ and Nd$_2$NiO$_{4+\delta}$ can be suppressed with a large excess of oxygen in the structure. It appears that F$^-$ in much smaller concentrations has a similar effect. Stoichiometric Nd$_2$NiO$_4$ shows an increase in the susceptibility around 120 K, which was attributed to the canting of the NiO$_6$ octahedra.

Conclusions

In summary, we have prepared fluorinated members of the solid solution series $Nd_{2-x}Sr_xNiO_{4+\delta}$ by a low temperature ion-exchange reaction. X-ray diffraction studies reveal that $Nd_2NiO_{4.16}$ undergoes considerable orthorhombic strain as a result of fluorination. Relative to the unfluorinated sample, the *a* cell parameter decreases while the *b* and *c* cell parameters increase. Energy dispersive X-ray analysis indicates that fluorine is uniformly distributed throughout the bulk of the sample. $Nd_2NiO_{4-x}F_y$ decomposes above 700°C into NiO, NdF_3, and NdOF. Electrical resistivity measurements indicate that the room temperature resistivity of selected $Nd_{2-x}Sr_xNiO_{4+\delta}$ increases upon fluorination. The metallic character seen for $NdSrNiO_4$ above 190 K is absent upon the incorporation of fluorine.

Acknowledgments

The authors thank Dr. Shu Li and Professor W. H. McCarroll for helpful discussions. The work was supported by National Science Foundation Solid State Chemistry Grant DMR-9019301.

References

1. J. M. Bassat, P. Odier, and F. Gervais, *Phys. Rev. B* **35,** 7126 (1987).
2. D. J. Buttrey, J. M. Honig, and C. N. R. Rao, *J. Solid State Chem.* **64,** 287 (1986).
3. C. N. R. Rao, D. J. Buttrey, N. Otsuka, P. Ganguly, H. R. Harrison, C. J. Sandberg, and J. M. Honig, *J. Solid State Chem.* **51,** 266 (1984).
4. D. J. Buttrey, and J. M. Honig, *J. Solid State Chem.* **72,** 38 (1988).
5. Hk. Müller-Buschbaum, *Angew. Chem. Int. Ed. Engl.* **28,** 1472 (1989) and references therein.
6. A. C. W. P. James, S. M. Zahurak, and D. W. Murphy, *Nature* **338,** 240 (1989).
7. Z. Kakol, J. Spalek, and J. M. Honig, *J. Solid State Chem.* **79,** 288 (1989).
8. K. S. Nanjundaswamy, A. Lewicki, Z. Kakol, P. Gopalan, P. Metcalf, J. M. Honig, C. N. R. Rao, and J. Spalek, *Physica C* **166,** 361 (1990).
9. J. D. Jorgensen, B. Dabrowski, S. Pei, D. R. Richards, and D. G. Hinks, *Phys. Rev. B* **40,** 2187 (1989).
10. J. Rodriguez-Carvajal, J. L. Martinez, J. Pannetier, and R. Saez-Puche, *Phys. Rev. B* **38,** 7148 (1988).
11. R. Saez-Puche, J. L. Rodriguez, and F. Fernandez, *Inorg. Chim. Acta* **140,** 151 (1987).
12. D. J. Buttrey, J. D. Sullivan, G. Shirane, and K. Yamada, *Phys. Rev. B* **42,** 3944 (1990).
13. R. Saez-Puche, F. Fernández, J. Rodríguez-Carvajal, and J. L. Martínez, *Solid State Commun.* **72,** 273 (1989).
14. P. Ganguly and C. N. R. Rao, *Mater. Res. Bull.* **8,** 405 (1973).
15. B. W. Arbuckle, K. V. Ramanujachary, Z. Zhang, and M. Greenblatt, *J. Solid State Chem.* **88,** 278 (1990).
16. B. L. Chamberland, *Mater. Res. Bull.* **6,** 311 (1971).
17. A. R. Storm, *Mater. Res. Bull.* **5,** 973 (1970).
18. F. F. Hubble, J. M. Gulick, and W. G. Moulton, *J. Phys. Chem. Solids* **32,** 2345 (1971).
19. A. Manthiram, X. X. Tang, and J. B. Goodenough, *Phys. Rev. B* **42,** 138 (1990).
20. P. Lightfoot, S. Pei, J. D. Jorgensen, X. X. Tang, A. Manthiram, and J. B. Goodenough, *Physica C* **169,** 15 (1990).
21. S. M. Zahurak, D. W. Murphy, S. Nakahara, W. W. Warren Jr., D. M. Krol, A. M. Thayer, D. C. Douglass, G. F. Brennert, S. H. Glarum, E. M. Gyorgy, S. M. Fine, and M. Greenblatt, *Solid State Ionics* **32/33,** 1104 (1989).
22. U. Lehmann and Hk. Müller-Buschbaum, *Z. Naturforsch. B* **35,** 389 (1989).
23. S. Tamura, *J. Phys. Soc. Jpn.* **33,** 574 (1972).
24. R. Saez-Puche, F. Fernandez, J. L. Martinez, and J. Rodríguez-Carvajal, *J. Less Common Met.* **149,** 357 (1989).